ISSN 0010-9525, Cosmic Research, 2018, Vol. 56, No. 5, pp. 343–351. © Pleiades Publishing, Ltd., 2018.
Original Russian Text © S.A. Semikov, 2018, published in Kosmicheskie Issledovaniya, 2018, Vol. 56, No. 5.

New Method of Recording Sunspots and Planets

S. A. Semikov*

Faculty of Radiophysics, Lobachevsky University, Nizhny Novgorod, 603950 Russia

**e-mail: sergey-semikov@yandex.ru*

Received March 22, 2017

Abstract—A new method for recording planets and searching for minor planets (asteroids), AISs, and satellites passing along the solar disk—an advanced method of Doppler tomography—has been developed. This method, due to its high sensitivity, will also allow one to detect exoplanets and specify elements of planetary orbits and the parameters of their stars. It can be used to determine the shape of stars and the distribution of surface brightness, as well as analyze the rotation of the star surface and its active regions (spots, flares, etc.). Finally, it will allow one to establish the shape of planets, AISs, and satellites passing along the star disk. It is based on analysis by high-resolution spectral devices of variations in the profiles of the emission and absorption lines of stars, broadened due to the rotation of stars or flows of emitting gases. For the use of high-resolution spectroscopies, new types of telescopes–spectrographs of record luminosity and a scheme of a mirror collimator–condenser are proposed. Possible manifestations of the Ritz effect in these measurements are considered.

DOI: 10.1134/S0010952518050064

INTRODUCTION

At present, detecting sunspots and planets passing along the solar disk is not difficult for astronomy. However, tracking the passage of minor planets (asteroids), comets, small spots along the solar disk, and monitoring spacecraft (satellites, AISs, etc.) presents a certain difficulty. In addition, this process of constant monitoring is rather difficult to automate, considering the need to process two-dimensional images on which real objects should be singled out from noise effects. In this paper, a new transit method for detecting planets and sunspots has been developed which can be used to search for exoplanets during transits, as well as to monitor variations in the shape and distribution of the surface brightness of stars.

The method is based on the study of the profile of the absorption lines of the Sun (or any other star) by high-resolution spectral instruments and is the development of the method of Doppler tomography [1]. Due to the effect of Doppler broadening of the lines caused by the axial rotation of a star, i.e., spread and dispersion of radial velocities along the star disk, a separate spectral line acquires a profile, each point of which approximately corresponding to the longitude or impact parameter of the corresponding points of the star. Since the circumferential equatorial velocity of stars reaches ~10–100 km/s, the width of the line profile reaches $\Delta\lambda_m \sim 1$ nm = 10 Å (for the Sun $V_r = 2$ km/s and $\Delta\lambda_m \sim 0.1$ Å), i.e., can be accurately measured by high-resolution spectral instruments. The passage (transit) of a planet or spot along the star disk is accompanied by a decrease in the intensity of the section of the profile of the absorption line or emission at the corresponding longitude with the corresponding radial velocity V_r. Thus, in terms of the shape of the profile and the motion of its parts, it is easy to detect the passage of planets and spots along the star disk determining their longitudes and, as we will further show, the latitudes, to determine orbit elements, dimensions, velocity, period, etc. In this case, data processing on computers is much simpler, since the line profile is easily recorded and can be quickly automated, in contrast to the case of the much more complex and longer processing of two-dimensional images.

Until now, a similar method of searching for exoplanets [1, 2] and star spots [3] discovered several years ago has found limited application due to its low sensitivity. In this paper, the theoretical foundations of the method are developed and schemes of optical systems are proposed to increase its sensitivity.

JUSTIFICATION OF THE METHOD FOR STUDYING LINE PROFILES

Let us consider a star in the form of a sphere that rotates with angular velocity ω and has radius R; in this case, the axis of rotation is perpendicular to the line of sight $\mathbf{r}$ (Fig. 1). In this case, the radial velocity at the edges of the star (at the equatorial points on the star limb) will reach the extreme values $V_r = \pm\omega R$. At other points on the star disk, the radial velocities take the intermediate values $-\omega R < V_r < \omega R$. Conditionally, we

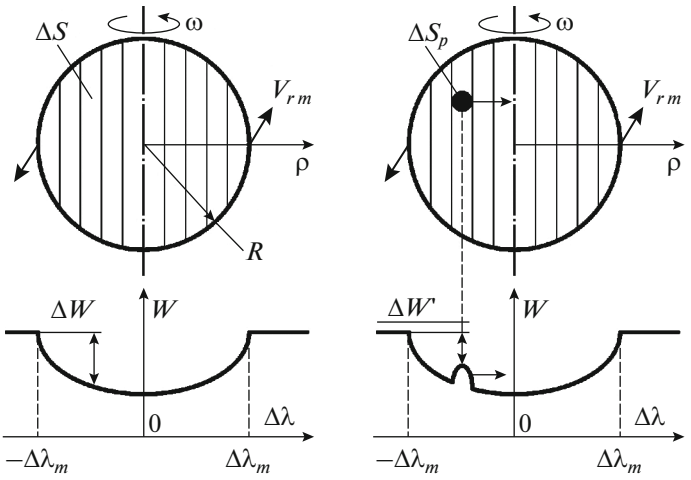

Fig. 1. Scheme of the star rotation and broadening of the profile of absorption line: in the case of a pure star disk (left) and partially covered by the planet's shadow or a star spot with an area of ΔS_p (right). As the spot or disk of the planet moves along the disk, the local maximum on the spectrum is shifted accordingly.

divide the star disk into strips parallel to the axis of rotation and displaced from it in the projection onto the picture plane at different distances ρ (we direct the ρ axis to the right). In this case, it is easy to show that the radial velocity of points within the strip is $V_r = \omega\rho$. Accordingly, due to the Doppler effect and the dispersion of the radial velocities over the star disk ($\Delta V_r = 2\omega R$), the profile of absorption line according to the Doppler effect broadens and acquires a shape roughly corresponding to the distribution of the intensity of absorption lines along the star disk. This is true if the broadening $2\Delta\lambda$ due to the spread (dispersion) of radial velocities ΔV_r is much larger than the intrinsic line width $\delta\lambda$ in the sections with $V_r \approx 0$. For most lines, for example, for the Sun, this condition is practically not fulfilled in view of the line broadening due to pressure, temperature (chaotic Doppler broadening), and individual surface motions—including due to convection in granules. However, in the spectrum of the Sun and other slowly rotating stars, one can find individual narrow lines for which the condition is satisfied. In addition, the condition is usually satisfied for stars with high circumferential velocities ($V \sim 100$ km/s), for example for Altair [4] and other rapidly rotating stars [1, 2].

Since under these conditions the intensity of the section of the absorption line corresponding to a certain radial velocity V_r is approximately proportional to the area dS of the luminous surface (strip) with this velocity in the interval from V_r to $V_r + dV_r$, we find that the profile of absorption line $\Delta W(\Delta\lambda)$ or emission will be an approximately repeated shape of the star disk. That is, the profile of absorption line $\Delta W(\Delta\lambda)$ will be, in the first approximation, a half-arc shape of the circle, an ellipse, if we do not take into account the darkening to the edge of the star (darkening to the edge is usually small for red and infrared rays [5]), as well as an increase in the thickness of the layer of chromosphere of the star, which passes by the light beam and which partly compensates the effect of darkening to the edge. Indeed, for rapidly rotating stars, for example in Altair, the profile of the spectral lines has an approximately elliptical shape [4] (Fig. 1). If we take into account the darkening to the edge of the disk, the variation in the path of light in the chromosphere of the stars, and the differential rotation and the initial width of the profile of the line $\delta\lambda$ (in the sections with $V_r \approx 0$), the shape of the profile will differ from the circular one. It is possible to reconstruct the shape of the profile due to rotational broadening alone if these effects are taken into account and the processing of the profile on the computer is carried out with the corresponding corrective corrections.

Indeed, it is known that the profiles of the lines of rapidly rotating stars, such as Altair and Ahernar, have the form of a semicircle—a semiellipse [1, 2]. However, for the rapidly rotating stars observed from the pole, for example for Vega, the profile is more complicated [4]. Indeed, when observing almost along the axis of rotation, ΔV_r decreases and the line intensities increase substantially at the center of the profile corresponding to the pole with $V_r \approx 0$, due to the excess of surface brightness in the polar regions according to the von Zeipel theorem [6]. In the case of noticeable darkening to the edge or in the case of a significant deviation of the shape of the star from the ellipsoid of rotation (for example, due to tidal effects), the profile of the absorption lines will be significantly distorted and will differ from the semicircle. Thus, even without the use of complex techniques of optical interferometry (telescopes–interferometers), one can determine, using only the profile of the absorption lines, the shape of the star disk and the inhomogeneity in the distribution of the surface brightness.

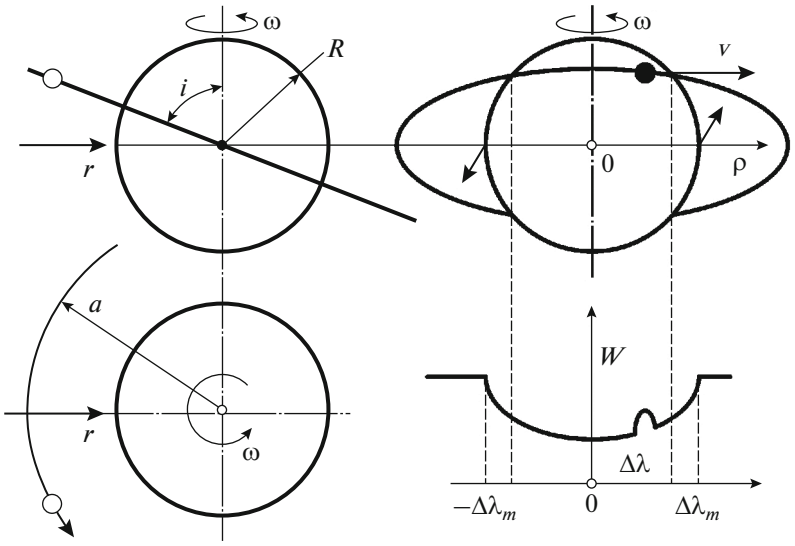

Fig. 2. To the calculation of the orbital elements of the planet with an inclination different from $i = 90°$.

Since a partial eclipse, a darkening of the star disk caused by a planet or star spot, leads to a decrease in the area of the strip corresponding to the certain value of V_r, the intensity in the profile of the absorption line will change accordingly. A local maximum appears on the profile of the absorption line (Fig. 1), the position and displacement velocity of which can detect planets and establish their coordinates, elements of orbit, and the transverse velocity v of their passage through the star disk. Indeed, similar variations in the profile of the absorption lines when passing exoplanets along the star disc are observed in the form of local maximum moving along the profile of line, allowing one to investigate the parameters of the motion of exoplanets using the so-called Doppler tomography method [1, 2]. A similar method allows one to record also the motion of stellar spots [3].

Since the profile of absorption lines is usually cut by noise, singling out maximum corresponding not to noise, but to the passage of a planet, is possible by changing the position of the maximum on the line profile $\Delta\lambda(t) \approx kvt$, where k is a constant. Unlike random noise, the signal from the passage of a sunspot or a planet is almost constant and the maximum from the planet is shifted along the spectral profile towards long waves with an almost constant rate $d\Delta\lambda/dt \approx kv$ (in the case of the direct motion of the planet), or with the harmoniously varying velocity $d\Delta\lambda/dt \approx k\omega R\cos(\omega t)$ in the case of spot motion, when t is counted from the instant of passage of the spot through the axis of symmetry of the disk (on the meridian with $\rho = 0$). This will make it easy to separate the signal from random noise on the profile of absorption line.

Indeed, the period of recurrence of maxima moving along the profile with a certain "velocity" $d\Delta\lambda/dt$ is equal to the orbital period P of the planet or the period of revolution T of the spot on the star disk associated with the rotation of the star surface. The time of eclipse Δt, if the planet passes along the equator of the star, will allow us to find the ratio between the orbital radius (the semiaxis a) and the equatorial radius of the star R (in the case of circular orbit): $a/R = P/\pi\Delta t$.

Thus, knowing the radius R of the star, for example from astrometric measurements, one can determine the radius of the star orbit a (Fig. 2). The passage of the planet along the equator of the star is detected by the fact that the maximum passes the entire width of the profile $2\Delta\lambda_m$ from the left to the right edge. This means that the inclination of the planetary orbit $i = 90°$. If the maximum motion begins not from the edges of the profile $\pm\Delta\lambda_m$, but from the intermediate sections $\Delta\lambda$ corresponding to the intermediate radial velocities of the star surface, then the inclination of the orbit is different from $i = 90°$. If $a \gg R$, assuming that the planet motion occurs along the star disk with constant velocity v, we obtain for the length 2ρ traversed along the disk, as well as for the section of the spectrum traversed along the profile of line, $2\Delta\lambda = 2\rho\Delta\lambda_m/R$, where $a/\rho = P/\pi\Delta t$. Hence, using trigonometry it is easy to determine the inclination of the orbit

$$i = \arccos\left(\frac{\pi\Delta t}{P}\sqrt{\Delta\lambda_m^2/\Delta\lambda^2 - 1}\right).$$

The ratio of the radius of the orbit to the radius of the star, in general, is found as

$$\frac{a}{R} = \frac{\Delta\lambda P}{\Delta\lambda_m \Delta t\pi}.$$

If the moving maximum on the profile is due to the motion of the solar (stellar) spot, then using the beginning of the transit from the section spaced from the center of the profile by $\Delta\lambda$, it is easy to find the latitude

of the spot $\varphi = \arccos(\Delta\lambda/\Delta\lambda_m)$. Indeed, the passage of spots along the star discs is clearly recorded by variations in the shape of the profiles of absorption lines [3].

In the case, if the motion of the planet takes place in an elliptical orbit, it is easy to determine the eccentricity and longitude of the periastron of the orbit according to the variation in the velocity of the motion of maximum along the profile of the absorption line. In addition, combining this method with the method of radial velocities using the Doppler shifts of the spectral lines, it is easy to refine these elements and compare them with the values found by other methods.

The dimensions of the planet or the spot are also elementally determined by the intensity of the maximum formed on the profile of the spectral line. Indeed, the spectral intensity of the absorption line ΔW (this can be determined as the local depth of the absorption profile, Fig. 1) is proportional to the area of the strip ΔS with a width equal to the diameter of the spot or planet. Assuming that within this strip the radial velocity and the surface brightness are constant (i.e., at constant proportionality coefficient u), we find $\Delta W\Delta\lambda = u\Delta S$.

Therefore, the eclipse of the section of the strip by the planet disk or spot with area ΔS_p leads to a decrease in the average intensity $\Delta W'$ of the section of the absorption line with a width $\Delta\lambda_p$ (within which a local maximum is observed) with respect to the initial intensity of the section of absorption line ΔW proportionally

$$\Delta W'/\Delta W = (\Delta S - \Delta S_p)/\Delta S.$$

Thus, it becomes possible to accurately measure the elements of the orbits and the dimensions of celestial bodies or spots passing along the visible star disk. The proposed method is most effective for celestial bodies, spots, and AISs passing along the solar disk, since the emission spectrum and the absorption lines of the Sun are sufficiently intense, which will allow us to measure the profile of absorption lines with huge resolution. For the Sun, the profile of line differs markedly from the arc of the circle, the ellipse, in view of the relatively small circumferential equatorial velocity of the Sun ($V_r \sim 2$ km/s) and the considerable line broadening from other effects. Nevertheless, there is a noticeable profile broadening due to rotation, so that, when comparing computer processing with a distorted (for eclipse) and undistorted profile of spectral lines, it is possible to determine the position of the planet, spot, satellite, and AIS and their motion. The exact theory of this effect is considered in more detail in [1, 3].

In addition, using the profile of the local maximum and its variation in the time interval between the first and second instants of contact with the limb of the star, it is possible to roughly determine the shape of the eclipsing planet or spacecraft (AIS, AES), for example, assuming their shape to be symmetric. This will allow one to identify the spacecraft by its dimensions and shape, similar to recognizing warships and aircrafts during wars only by their silhouette.

In the case of other stars, the light intensity is usually too small to measure in detail the spectral profile of the absorption line with a sufficiently high spectral resolution. Indeed, the emission energy within the width of one line is too small, and the profile cannot be measured in detail by the photometry method of the spectral region or the degree of blackening of the photographic plate sections. However, in this case, since it is not required to study a two-dimensional image, multimirror telescopes collecting light from a large area on the slit of a spectrograph without strict focusing can find use, which will provide a sufficient aperture ratio and resolution. In addition, since the profile for many lines is approximately the same (if we consider the lines formed in the chromosphere of the star), we can investigate the integrated emission power from a number of such spectral lines by collecting their images into one on one photodiode ruler or photographic plate (Fig. 3). Thus, by increasing the aperture ratio, a huge frequency resolution (wavelength λ) can be achieved when studying the shape of the profile of the absorption lines. Indeed, the specific wavelength λ, on which the profile is studied, is not that significant, since in all formulas of the proposed method the relative widths and coordinates of the line profiles $\Delta\lambda/\Delta\lambda_m$ appear.

ASTROSPECTROGRAPH OF ULTRAHIGH SPECTRAL RESOLUTION

The spectrograph for a detailed study of the profiles of the spectral lines of the Sun and stars can be constructed as follows. A system of flat mirrors with an electromechanical drive distributed over the large area (~1 km^2) and synchronously controlled by computers collects parallel rays of light from the star into the narrow aperture at the top of the measuring tower observatory. Then the light beam, passing through the collimator–condenser, is collected on the slits of the spectrograph, which decomposes light into the spectrum (Fig. 3). This spectrum is projected onto the screen in the form of a mask (transparency) with slots opposite the absorption lines. Then the short sections of the spectrum that pass through these slits are directed to the oppositely oriented prism or diffraction screen, which again collects the spectrum into a parallel beam and, through the lens, focusses into a narrow section on the photodiode ruler (or photomultiplier ruler) of the spectrometer, or on a photographic plate to measure in conditions of long exposure. If the rays simply passed through the slits in the mask (transparency), they would be focused in one line (in the shape of the input slit of the spectrograph). However, since it is required to obtain the profile of absorption lines by simply combining different lines, it is necessary to put a narrow collecting cylindrical lens after each slot of the mask–transparent, defocusing each beam, so that

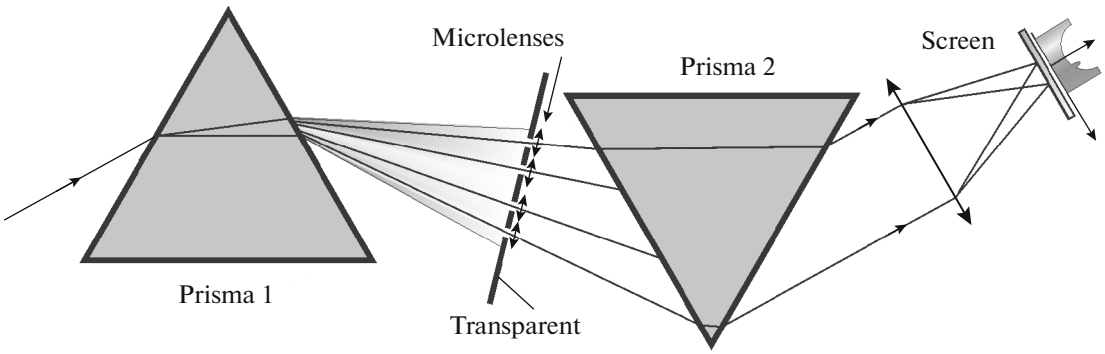

Fig. 3. Scheme of the spectrograph for studying the integral profile of spectral lines.

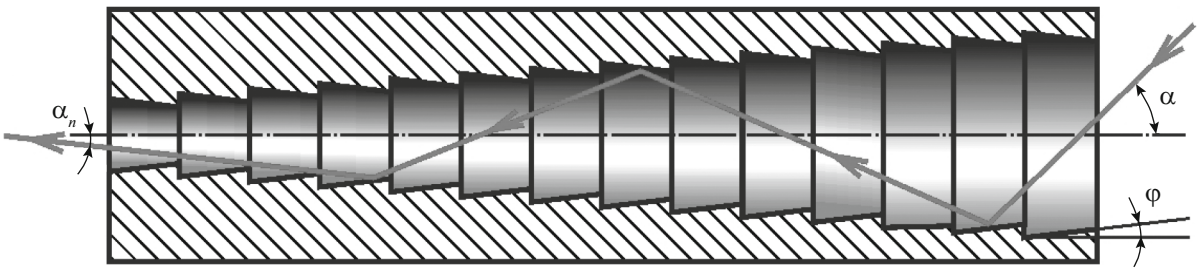

Fig. 4. Scheme of the universal collimator–condenser of light.

on the spectrometer or photographic plate the light from each slot is focused not in a line, but in a strip whose edges correspond to the edges $\pm\Delta\lambda_m$ of the spectral profile of the lines. In this case, the integral profile of the line will be obtained if the focal lengths of the lenses are selected in such a way that the edges of the profiles coincide at the coincident spectral lines (Fig. 3). Accordingly, the intensity of the integral profile will be appreciably higher than for each individual line, which will make it possible to accurately measure the profile of absorption lines at high spectral resolution.

A condenser, which collects light beams on the spectrograph slits, must also be specifically constructed. Since the focusing system of the astrospectrograph collects separate parallel beams of light from plane mirrors into one aperture, they cannot be assembled by any focusing system into one point. However, since it is not necessary to obtain a correct two-dimensional image, the beams should be sufficiently approximated into one parallel beam, and then the lens should be focused to the point on the spectroscope slit. This collimation of the beams can be achieved by means of a funnel-like mirror collimator–condenser (Fig. 4), which is an axisymmetric surface consisting of a series of successive annular conical mirrors with a generatrix almost parallel to the axis of the collimator (with an angle $\varphi \sim 1°$) and facing the output end of the device. That is, the collimator must be made in the form of a surface of revolution resembling a cocktail tube.

If the initial ray falls at angle α to the axis of the collimator, then for each subsequent reflection from the walls of the collimator this angle decreases by 2φ, so that after the nth reflection the angle to the axis for the reflected ray $\alpha_n = \alpha - 2\varphi n$. Thus, practically independently of that in which point and at what angle the rays enter the collimator, if the maximum angle of their input is equal to α, then, through $n = \alpha/2\varphi$ reflections, the incoming beam at the output of the collimator is converted into an almost parallel beam of rays, since $\alpha_n \approx 0°$. One important property of this collimator is that its collimation capacity increases with increasing angle α, since, with increasing α, the number n of reflections increases on the length L of the condenser. Thus, all rays are reduced to a parallel beam at approximately the same distance L from the point of input into the device. Another important difference from reflex and refractor systems is that the collimating capacity of the condenser is the same for the rays entering the aperture at different distances from the optical axis (the axis of symmetry of the collimator). This is what makes it possible to collect all rays into one parallel beam, regardless of the angle and the point at which they enter the system. With a large aperture size ($D \sim 1$ m) and $\varphi \sim 1°$, the length of the collimator needed to collect light into the parallel beam must be $L \sim D/\varphi$ (where φ is expressed in radians), whence $L \sim 60$ m. That is, the collimator must

have a large size and be located vertically in the tower of the observatory; i.e., the spectrograph at the output of the collimator is located at the base of the tower.

To increase the accuracy of collimation (to reduce the spread in the angles of the output of the rays), φ should be reduced. This ensures the collimation of the rays crossing the axis of the collimator or close to it. For the collimation and approach of the rays entering the aperture at a considerable distance from the axis (i.e., the rays crossing with the axis), the radius of the conical mirrors should gradually decrease as it approaches the output of the collimator. In this case, as the beam approaches the output, it will become not only closer to parallel, but will also narrow.

Then the narrow, almost parallel, paraxial beam is focused by the lens into the slit of the spectrograph. This collimator–condenser is unlikely to be used in optics to form correct images, because the individual rays in the beam are not phased: rays correspond to different lengths of optical paths, and they come out at several different angles α_n. However, this new type of collimator–condenser can find application as a system approximately collecting light.

INVESTIGATION OF EMISSION SPECTRA AND LINE PROFILES

The considered method of searching for planets while studying the profiles of emission lines will be even more effective. Indeed, the brightness of the emission lines in individual cases is comparable to the integral brightness of the celestial bodies themselves—the stars. In particular, the spectra of quasars contain very bright emission lines. It is not ruled out that, with increasing the spectral resolution in the emission spectrum, it will be possible to detect details that allow one to establish the detailed structure of quasars. In the spectrum of quasars, the so-called Lyman-alpha forest is found in the form of a fence of the Lyman-alpha spectral lines of hydrogen. It is customary to explain these lines by absorption in intergalactic gas clouds having intermediate velocities. However, it is possible that each line corresponds to a star or a group of stars. Then, for high spectral resolution, it will be possible to study the spectra and brightness variations of individual stars forming quasars. A significant difference in the red shifts of the spectral lines of the Lyman-alpha forest of quasars can be connected with the fact that the displacement is caused not by the Doppler effect, but by the hypothetical Ritz effect [7–11]. According to this effect, which follows from the ballistic theory of Ritz, an additional variation in the wavelength takes place due to the presence of the radial acceleration a_r in the stars. The transformed wavelength λ' and frequency f' are expressed in terms of the initial λ and f as

$$\lambda' = \lambda\left(1 + ra_r/c^2\right),\ f' = f/\left(1 + ra_r/c^2\right), \qquad (1)$$

where r is the distance to a star or quasar and c is the speed of light in vacuum.

Since for different stars the radial accelerations a_r of emitting and absorbing atoms differ both due to different radial orbital acceleration and due to the difference in the acceleration of free fall on the surface of different stars, the spectral lines acquire different red shifts that at distances r of quasars can be comparable with the value of the red shift of the quasar itself. Accordingly, because of the dispersion of the radial accelerations, a significant dispersion of the red shifts arises and, instead of a single emission or absorption line, a set of emission and absorption lines—the Lyman-alpha forest—is obtained. Note that the Ritz effect elementarily explains the significant red shift of quasars, which is not consistent with Hubble law, as well as explains the Hubble law itself, solving its paradoxes [7–11]. In addition, this hypothesis explains the significant relative width $\Delta\lambda/\lambda$ of the spectral lines for some quasars comparable with the red shift z. This alternative non-Doppler explanation of the cosmological red shifts in the spectra of galaxies has been repeatedly suggested by different authors, beginning with A.A. Belopolsky [7, 12] and F. Zwicky, and to the present time is supported by many astronomers [13].

The Ritz effect ceases to change the frequency only when light passes through relatively dense reemitting medium [9]. The reemission of light by interstellar gas is especially effective near the resonant frequencies of atoms. In the process of shifting the continuous spectrum according to the Ritz effect and flashing its energy at frequencies f' of spectral lines, for example, Lyman-alpha (L_α), there should be a sharp weakening of the continuous spectrum on the blue side of these lines at frequencies $>f'$. Then, after reemission at these frequencies, light will not vary the frequency according to the Ritz effect, and the continuous spectrum on the blue side of the line will abruptly terminate. This phenomenon is actually discovered as the Gunn–Peterson effect: at the blue boundary of the L_α line, the continuous spectrum abruptly terminates and, further in the shortwave region, a fringe of the absorption lines of the Lyman-alpha forest is observed [12, p. 390], which arise as a result of additional and noncoincident displacements of the L_α absorption lines. This effect resembles a laser: a continuous emission, whose spectrum is shifted by the Ritz effect, plays the pumping role, and the L_α spectral line plays the role of an emitting transition on which the pump energy is "eaten out"; the energy of the continuous spectrum is emitted at the frequency of this line. Therefore, further, beyond the L_α line, the continuous spectrum noticeably weakens and the Lyman-alpha forest is formed.

In the atmosphere of the Sun, the Ritz effect can also lead to a shift in the spectral lines, for example, due to the acceleration of the free fall of emitting atoms and electrons in the gravitational field of the Sun. However, if we take into account the relatively small

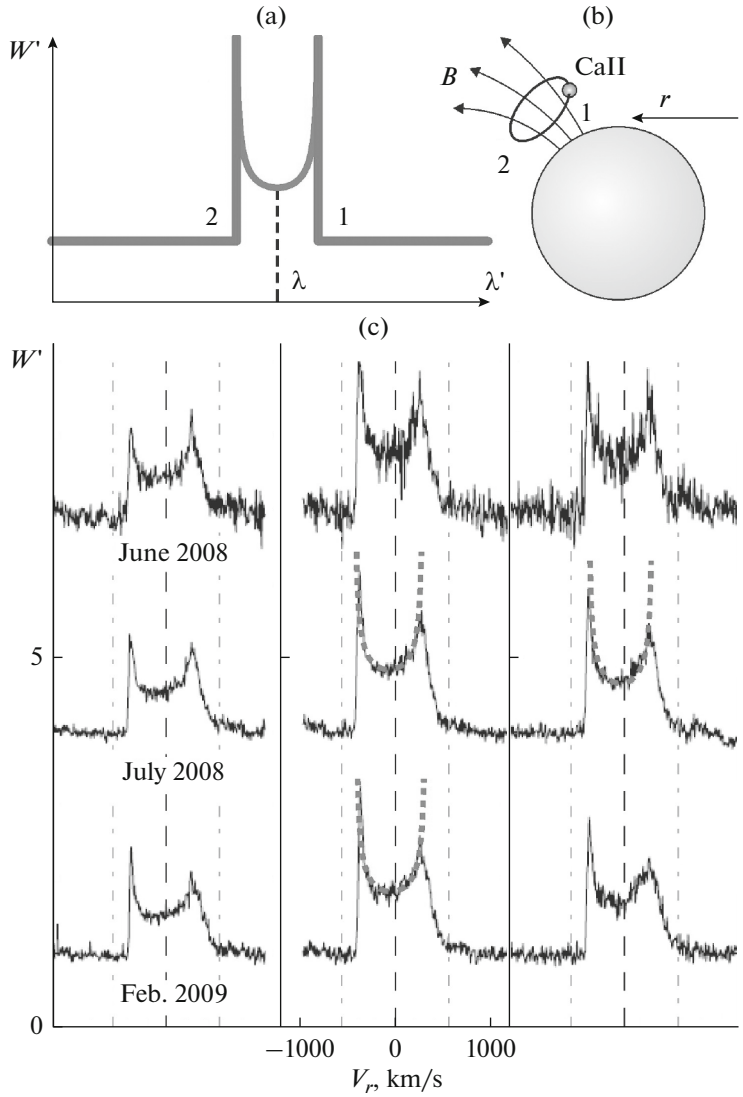

Fig. 5. Formation of the profile of the CaII emission lines when moving ions in the magnetic field *B* of the star: (a) the theoretical profile, (b) the circular orbit of ions in the *B* field of the star, (c) and the observed profiles of the CaII line in the SDSS J1228 + 1040 spectrum [16, 17]. The dotted line shows the theoretical profile of the lines.

(on astronomical scales) distance r to the Sun, these displacements are insignificant, making, if we take into account reemission in the solar atmosphere, $\Delta\lambda \approx 0.013$ Å. Thus, the Ritz ballistic theory gives an alternative explanation for the red shift of lines in the gravitational field of the Sun, an effect which, it was believed, can only be explained within the framework of the general theory of relativity [15].

In the case of emission lines, the profiles are more complex than absorption lines, which is associated with a more complex velocity distribution, since emission lines are created by gas flows emitted by stars with high velocity. Accordingly, the profile of the spectral lines becomes noticeably more complicated and distorted. In this case, emitting ions, for example, ejected during flares, move in the magnetic field of a star with high accelerations a_r and velocities $V_r \sim 100$ km/s under the action of the Lorentz force winding trajectories on the magnetic field lines (Fig. 5b). For simplicity, we assume that the motion under the action of the Lorentz force occurs along a circle (since the velocity component longitudinal to the field varies only the total line displacement, and not its profile); then the ion radial velocity varies with the time t according to the law $V_r(t) = V_m \sin(\omega t)$, where V_m is the amplitude of the radial velocity and ω is the cyclotron frequency of ions. Then the change in the wavelength of light according to the Doppler effect will oscillate according to the law

$$\Delta\lambda(t) = \lambda V_m \sin(\omega t)/c = \Delta\lambda_m \sin(\omega t).$$

The intensity of the profile section $Wd\lambda'$ is proportional to the exposure time dt of the line with the cor-

responding shift $\Delta\lambda$ and the wavelength $\lambda' = \lambda + \Delta\lambda$; i.e., $Wd\lambda' = wdt$, where w is a constant. Hence, the line profile, i.e., the spectral power density $W(\lambda')$, is

$$W(\lambda + \Delta\lambda) = w\frac{dt}{d\Delta\lambda} = \frac{w^*}{\sqrt{1 - \Delta\lambda^2/\Delta\lambda_m^2}}, \qquad (2)$$

where $w^* = wc/\omega\lambda V_m$ and $\Delta\lambda_m = \lambda V_m/c$. Indeed, the profile of the emission lines is characterized by just such a dovetail-like shape (Fig. 5), for example, for the white dwarf SDSS J1228+1040 [16, 17]. When interpreting the observed line profile [16] according the Doppler effect, ions should move at velocities of ~1000 km/s, which corresponds to the typical ion velocity in solar flares and stars. We note that this was exactly proposed in [16] to construct an image using the Doppler method, but instead of an apparent star disk, it was a ring surrounding the star of the gas disk.

Another possible reason for the broadening of the emission lines is the acceleration caused by the Lorentz force during the motion of emitting ions in the magnetic field of the star, leading, according to the Ritz effect (1), to a significant shift in the spectral lines alternately to the red and blue regions of the spectrum. When averaging over time and different velocities, this dispersion of the radial accelerations leads to the symmetrical line broadening observed in white dwarfs, a number of red dwarfs, and supergiants [4]. If the broadening was due to the dispersion of the radial accelerations of free fall on the star surface, it would be asymmetric, contrary to observations, according to which the absorption lines have a symmetrical profile. In the case of emission lines (for example, CaII ions) produced by local high-speed gas flows moving in the magnetic field of a white dwarf, the profile acquires a more complex shape, with two sharp peaks at the edges [16]. This form of the profile, from the point of view of the Ritz effect, can be derived in the same way as when deriving the formula for profile (2) calculated from the Doppler effect. If the radial acceleration a_r of each ion is formed of the free-fall acceleration a_g and the acceleration a_m from the Lorentz force, we find $a_r = a_g + a_m\sin(\omega t)$, where ω is the cyclotron frequency of an ion. As a result, taking into account the Ritz effect, we find the new wavelength $\lambda' = \lambda(1 + ra_r/c^2) = \lambda + \Delta\lambda$, where $\lambda = \lambda_0 + \lambda_0 ra_g/c^2$ is the average wavelength of the line, $\Delta\lambda = \lambda_0 ra_m\sin(\omega t)/c^2$ is the rapid variable correction to the wavelength, and λ_0 is the initial wavelength. Hence, the line profile, i.e., the spectral power density, is given by the same Exp. (2) as in the case of Doppler broadening. However, in this case, in Exp. (2), we should take $w^* = wc^2/\omega\lambda_0 ra_m$, but $\Delta\lambda = \lambda_0 ra_m/c^2$. As was noted, the profile of the emission lines observed in some stars is characterized precisely by this form [16, 17].

During the axial rotation of the star and the active region emitting energetic ions located at a fixed longitude, the angle of inclination of the ion orbit in the magnetic field varies to the line of sight and the value of the maximum radial accelerations a_m and velocities V_m. Accordingly, the width of the profile will vary periodically. If an eclipse occurs in individual parts of the trajectory of ions by a star (Fig. 5), the profile will be distorted, weakening at the longwave or shortwave edge of the profile. Indeed, such profile distortions are observed [16, 17]; in this case, the cut-out part of the profile just corresponds to the rounded shape of the star.

CONCLUSIONS

As was shown in the paper, the proposed method for studying the fine features of the profiles of emission and absorption spectral lines will make it possible to refine the parameters of the motion of the active sections of the solar and stellar surfaces in the photosphere and the characteristics of the gas motion in the chromosphere of the star without resorting to methods of conventional telescopy. Also, the new method will make it possible to clarify the fine features of the motion of the details of the stellar surface (sunspots, flares, etc.). In addition, the new method of searching for planets, exoplanets, AIS monitoring, and satellites, which is an advanced method of Doppler tomography [1, 2], will allow one to elementarily record the passage along the solar disk of not only planets, but also comparatively small bodies, asteroids, comets, AISs, satellites, etc., and, in the case of other stars, the passage along the discs of stars of exoplanets, additionally specifying the elements of orbits [11]. This will allow us to more accurately calculate the elements of the orbits of the corresponding celestial bodies and AISs, supplementing information on it obtained by other methods, methods of photometry, radial velocities, etc. One particularly effective method will be the method for studying stars of small diameter, for which the relative variation in the luminous area is higher than for large stars, which will permit one to record the passage of small celestial bodies along the star discs.

The results of this work have been reported at the 21st Scientific Conference on Radiophysics at Nizhny Novgorod State University [18] and are further substantiated by the author in the materials of the Ph.D. thesis [19].

ACKNOWLEDGMENTS

I thank Prof. M.I. Bakunov, Nizhny Novgorod State University, for discussing issues related to the features of wavelength-spectral transformation of the lines, as well as V.V. Kocharovsky and G.B. Malykin, employees at the Institute of Applied Physics, Russian Academy of Sciences.

REFERENCES

1. Cameron, C., Bruce, V., Miller, G., et al., Line-profile tomography of exoplanet transits: 1. The Doppler shadow of HD 189733b, *Mon. Not. R. Astron. Soc.*, 2010, vol. 403, no. 1, pp. 151–158.
2. Marshall, J., Cochran, W., Cameron, C., et al., Measurement of the nodal precession of WASP-33 B via Doppler tomography, *Astrophys. J. Lett.*, 2015, vol. 810, id L23.
3. Böhm, T., Holschneider, M., Lignieres, F., et al., Discovery of starspots on Vega, *Astron. Astrophys.*, 2015, vol. 577, id A64.
4. *Fizika kosmosa* (Space Physics), Moscow: Sovetskaya entsiklopediya, 1986.
5. Menzel, D.G., *Nashe Solntse* (Our Sun), Moscow: Fizmatlit, 1963.
6. Aufdenberg, J.P., Mérand, A., Coudé du Foresto, V., et al., First results from the CHARA array. VII. Long-baseline interferometric measurements of Vega consistent with a pole-on, rapidly rotating star, *Astrophys. J.*, 2006, vol. 645, no. 1, pp. 664–675.
7. Semikov, S.A., The Cosmos of the Russian Aristarchus, *Istor. Nauki Tekh.*, 2007, no. 1, pp. 60–64.
8. Mushailov, B.R. and Teplitskaya, V.S., On reliability of determining the orbital parameters of exoplanets by the Doppler method, *Cosmic Res.*, 2012, vol. 50, no. 6, pp. 421–430.
9. Semikov, S.A., Ob eksperimental'noi proverke ballisticheskoi teorii sveta, *Vestn. Nizhegorod. Gos. Univ.*, 2013, no. 4, pp. 56–63.
10. Semikov, S.A., The effect of light frequency transformation at source acceleration and criteria for its experimental verification, *Nelineinyi Mir*, 2014, no. 6, pp. 3–15.
11. Semikov, S.A., On the nature of the Barr effect and anomalous eccentricities of exoplanets, *Nelineinyi Mir*, 2016, no. 2, pp. 3–37.
12. Belopol'skii, A.A., *Astronomicheskie trudy* (Astronomical Works), Moscow: Gostekhizdat, 1954.
13. Mel'nikov, O.A. and Popov, V.S., NonDoppler explanations of the red shift in the spectra of far galaxies, in *Nekotorye voprosy fiziki kosmosa, 2* (*Some Issues in Space Physics, 2*), Moscow: VAGO AN SSSR, 1974, pp. 9–32.
14. *Galaktiki* (Galaxies), Surdin, V.G., Ed., Moscow: Fizmatlit, 2013.
15. Vavilov, S.I., *Sobranie sochinenii* (Collection of Works), vol. 4, Moscow: AN SSSR, 1956, p. 96.
16. Mancer, C.J., Gänsicke, B.T., Marsh, T.R., et al., Doppler imaging of the planetary debris disc at the white dwarf SDSS J1228+1040, *Mon. Not. R. Astron. Soc.*, 2016, vol. 455, no. 4, pp. 4467–4478.
17. Hartmann, S., Nagel, T., Rauch, T., et al., The gaseous debris disc of the white dwarf SDSS J1228+1040, *Astron. Astrophys.*, 2016, vol. 593, id A67.
18. Semikov, S.A., *Metody eksperimental'noi proverki ballisticheskoi teorii Rittsa* (Methods for the Experimental Verification of Ritz's Ballistic Theory), Nizhny Novgorod: Kirillitsa, 2017.
19. Semikov, S.A., A new type of collimators and high-aperture spectrographs for measuring the profile of spectral lines, in *Trudy XXI nauchnoi konferentsii po radiofizike, 10–13 maya 2017 g.* (Proceedings of the XXI Scientific Conference on Radiophysics, May 10–13, 2017), Nizhny Novgorod: NNGU, 2017, pp. 284–287.

Translated by N. Topchiev